Toward an accurate determination of half-life of ^{147}Sm isotope*

Odilon A. P. Tavares[1] and Maria Letizia Terranova[2]

[1]Centro Brasileiro de Pesquisas Físicas–CBPF/MCTIC, Rua Dr. Xavier Sigaud 150, 22290-180 Rio de Janeiro-RJ, Brazil

[2]Dipartimento di Scienze e Tecnologie Chimiche, Università degli Studi di Roma "Tor Vergata", via della Ricerca Scientífica s/n, 00133 Roma, Italy

E-mail: terranova@roma2.infn.it

PACS: 21.10.-k, 23.60.+e, 27.60.+j, 91.80.-d

Keywords: alpha decay, ^{147}Sm isotope, half-life determinations, geochronological applications

Abstract

The task of an accurate determination of alpha-decay rate of ^{147}Sm isotope, a topic of importance for both basic and applied science, has been faced in the present research following two different routes. First, a critical review and data analysis of the whole set of half-life-values obtained up today that yielded a value of (106.3 ± 0.5) Ga. Second, a one-parameter, semi-empirical model for alpha emission from nuclei, developed in the framework of the quantum mechanical tunneling mechanism through a Coulomb-plus-centrifugal-plus-overlapping potential barrier, that yielded a value of (108.2 ± 3.0) Ga. The good agreement found between the half-life values obtained from these procedures represents a net progress towards the assessment of a reliable ^{147}Sm alpha-decay rate to be used in geo- and cosmo-chronological investigations.

*Accepted for publication in Applied Radiation and Isotopes on April 03, 2018.

1. Introduction

The strong increase of interest towards the whole class of Lanthanides, also called Rare Earths Elements (REE) is due to the fact that such elements are nowadays of fundamental and, sometimes, vital importance in many technological fields, from consumer electronics to communications, from clean energy to health care, advanced transportation, security and more. The concerns over the supply chain and future availability of REE, however, led many countries (USA, EU, Japan) to insert the natural elements of the 4*f* transition series of the Periodic Table inside the class of "critical elements" [1−3].

Samarium and Neodymium have very similar ionic radii and valences and, therefore, a rather identical chemical behavior. This means that Sm/Nd systems suffered slightly from the modifications of the thermodynamic equilibrium conditions occurring during the growth of the terrestrial planets and retained their structural organization also during metamorphic processes in ores and meteorites. For these reasons, techniques based on couples of Sm and Nd isotopes, proposed starting from the 1970's, have nowadays grown into essential tools for geological and mineralogical dating [4−10].

As regards the issue of cosmochronology, the radioactivity of nuclides of extremely low decay rates is a powerful methodology for measuring cosmic times [11, 12]. In effect, the signatures of long-lived primordial isotopes, formed in the build-up of the solar system matter, and still present in planetary materials, is expected to provide important constraints on the current paradigm of the solar system formation. To this aim, in their pioneering research work, Fowler and Hoyle proposed ^{238}U-^{232}Th and ^{235}U-^{238}U systems [13]. After that, methodologies based on radioactivity of ^{87}Rb, ^{147}Sm, ^{187}Re, ^{232}Th, ^{238}U and ^{235}U isotopes have been applied [14−16].

The study of long-lived radionuclides helps to paint a picture of the nucleosynthetic events, to determine the mean age of elements and to elucidate the scenario of galactic evolution, as demonstrated by the reliable results obtained for the age of Earth and meteorites [17, 18], the solar system [19-23], and for some stars in our Galaxy [24,25].

Samarium has two alpha-decaying nuclides, ^{147}Sm and ^{148}Sm, but this latter is characterized by a half-life ~10^{16} a, that does not allow to measure with

precision the production of the daughter isotope ^{144}Nd, whereas isotope ^{147}Sm is quite suitable for applications in cosmochronology, because its decay into ^{143}Nd stable isotope is characterized by an easily measurable half-life of almost one order of magnitude (~7.7) greater than the age of the Universe (13.82 Ga) [26].

The ^{147}Sm→^{143}Nd system is thus a good candidate for dating [4,27], and particularly suitable for chronological studies of ancient ores and meteorites, witnesses of the earliest cosmic times when agglomeration of micrometer-sized dust produced by nucleosynthesis evolved in the macro-sized components of the earth's matter [28-30]. However, this application is not free from difficulties, because it needs a very accurate determination of the half-life of the ^{147}Sm radiogenic parent nucleus.

Starting from the pioneering studies by Hevesy *et al.* [31, 32] and Curie and Joliot [33], a long series of measurements of the alpha radioactivity of ^{147}Sm has been performed up to the present days [34], yielding half-life-values spanning between (94 ± 8) Ga [35] and (125 ± 6) Ga [36], (see Table 1 and references therein).

The discrepancies among the experimental data can be rationalized by considering that both the low abundance of ^{147}Sm in ^{nat}Sm (14.99%), and the low decay counting rate for such long-lived isotope (~7 $min^{-1}mg^{-1}$ and ~50 $min^{-1}mg^{-1}$ for ^{nat}Sm and ^{147}Sm, respectively) determine systematic uncertainties. Moreover, the data reported in literature have been obtained using different experimental techniques as well as a variety of detection methodologies with variable registration efficiency.

To overcome the drawback related to some of the techniques used in past experiments, very recently a high precision measurement of the alpha decay half-life of ^{147}Sm has been carried out by Wilsenach et al [34], taking advantages of morphological, structural and compositional improved techniques typical of the material science. The combined use of ICP-MS (inductively coupled plasma mass spectrometry), RBS (Rutherford back-scattering), EDX (energy-dispersive x-ray spectroscopy), TEM (transmission electron microscopy), AFM (atomic force microscopy) and TF-GIC (twin Frisch-grid ionization chamber) allowed Wilsenach *et al.* to attain for the half-life of ^{147}Sm the value of (107.9 ± 2.6) Ga [34].

In view of the geo- and cosmo-chronological applications, today a precise and accurate determination of the ^{147}Sm decay rate is becoming of fundamental importance, because even a little uncertainty in the data can severely hamper the applicability of the ^{147}Sm→^{143}Nd dating system. In this context, it was felt that a key tool to define a reliable value for half-life of ^{147}Sm isotope would be to re-analyze all the existing data, in the frame of methodology that accounts for the different techniques of measurement and geochronological inter-comparisons as well.

To corroborate the value obtained from the statistical treatment, it seemed worthwhile to perform also an evaluation of ^{147}Sm half-life using a physical model able to describe quantitatively the spontaneous alpha-particle emission mechanism from atomic nuclei. A one-parameter model based on the quantum mechanical tunneling mechanism through a Coulomb-plus-centrifugal-plus-overlapping potential barrier, constructed within the spherical nucleus approximation, was successfully used in the past to evaluate the alpha-decay half-lives of the naturally occurring ^{209}Bi and all the possible Bi isotopes that could be produced by nuclear reactions [62]. The success of such calculation method prompted us to follow the same methodology for a semi-empirical evaluation of ^{147}Sm half-life.

In the present work we compare the output of the statistical analysis performed of the whole set of ^{147}Sm alpha-decay experimental data with the estimated value obtained in the frame of the one-parameter model and make considerations about the recommended value of the ^{147}Sm half-life to be used for geo- and cosmochronological investigations.

2. Treatment of the measured half-life-values of ^{147}Sm isotope

We report in Table 1 a list of thirty-four measured values for the half-life of ^{147}Sm isotope.

Table 1. Measured values for half-life of ^{147}Sm isotope

Year of publication	Author(s)	Experimental method	Half-life $T_{1/2}$ [Ga]	Ref.
1933	G. Hevesy *et al.*	Geiger-Müller counter	180[a]	[32]
1934	M. Mader	Ionization Chamber	150[b]	[37]
1934	W. F. Libby	Geiger-Müller counter	94 ± 8[a]	[35]

1934	D. Lyford		106 ± 7[a,c]	[38]
1934	M. Herszfinkiel and A. Wroncberg	Ionization Chamber	200 ± 10[a]	[39]
1934	M.Curie and F. Joliot	Wilson Chamber	150[a]	[33]
1936	R. Hosemann	Gamma detector plus Wilson Chamber	150 ± 11[a]	[40]
1937	H. Bethe	From data reported on page 166 of [Bet37]	194[a]	[41]
1947	C.M.G. Lattes *et al.*	Nuclear-track emulsion	140 ± 10[a]	[42]
1949	E. Picciotto	Nuclear-track emulsion	100 ± 6[a]	[43]
1954	G. E. Leslie	Nuclear-track emulsion	115 ± 3	[44]
1954	G. Beard and M.L. Wiedenbeck	Proportional counter	125 ± 6	[36]
1958	G. B. Beard and W.H. Kelly	Samarium-loaded liquid scintillator	106 ± 4[d]	[45]
1960	M. Karras and M. Nurmia	Ionization Chamber	114 ± 5	[46]
1961	P. M. Wright *et al.*	Liquid Scintillation Counter	105 ± 2	[47]
1961	R. D. MacFarlane and T. P. Kohman	Ionization Chamber	115 ± 5	[48]
1961	G. Graeffe and M. Nurmia	α-spectrometry with thick source	113 ± 3[e]	[49]
1964	D. Donhoffer	Liquid Scintillation Counter	104 ± 3	[50]
1965	K. Valli *et al.*	Ionization Chamber Liquid Scintillator Counter	108.3 ±2.0 107.5 ± 1.5	[51]
1970	M. C. Gupta and R. D. MacFarlane	Ionization Chamber	106 ± 2	[52]
1978	G.W. Lugmair and K. Marti	Geochronological Inter-comparisons	106.0 ± 0.8	[5]
1987	B. Al Bataina and J. Janecke	Proportional counter	105 ± 4	[53]
1992	J. B. Martins *et al.*	CR-39 nuclear-track detector	106 ± 4[f]	[54]
1992	G.W. Lugmair and S. J. G. Galer	Geochronological Inter-comparisons	106.1 ± 0.4	[55]
2003	N. Kinoshita *et al.*	Silicon-surface barrier detector Liquid Scintillator Counter	117 ± 2 115 ± 2	[56]
2009	K. Kossert *et al.*	Liquid scintillation Counter	107.0 ± 0.9	[57]
2010	J. Su *et al.*	Sm metal with silicon-surface barrier detector	106 ± 1	[58]
2010	J. Su *et al.*	Sm oxide with silicon-surface barrier detector	107 ± 1	[58]
2017	H. Wilsenach *et al.*	Twin Frisch-grid Ionization Chamber	115.4 ± 3.4[g]	[34]
2017	H. Wilsenach *et al.*	Twin Frisch-grid Ionization Chamber	107.4 ± 4.3[g]	[34]

2017	H. Wilsenach *et al.*	Twin Frisch-grid Ionization Chamber	112.5 ± 3.7[g]	[34]
2017	H. Wilsenach *et al.*	Twin Frisch-grid Ionization Chamber	106.9 ± 1.0[g]	[34]

[a] Corrected for 15% of ^{147}Sm in ^{nat}Sm.
[b] Quoted in [47].
[c] Quoted in [59]; uncertainty of 7% attributed.
[d] Corrected as quoted in [60].
[e] Uncertainty of 3% has been attributed.
[f] Corrected for the fraction of 0.8624 of natural Samarium in the oxide Sm_2O_3 (see [61]).
[g] Measurement with the sample on a silicon holder.

The compilation of Table 1 has been made taking advantage of the experimental results reported in Refs. [34, 57, 58, 60, 61, 63, 64] as well as in other literature sources. An uncertainty of ~7% was attributed to some measurements [38, 40, 42], while an uncertainty of about ~3% was attributed to the result reported in [49].

Since only in 1950 it was established that ^{147}Sm isotope was the source of alpha particle emitted from ^{nat}Sm [65], the decay rates measured up to that time were determined by considering the total amount of samarium samples, not the 15% of ^{147}Sm present in the isotopic composition of ^{nat}Sm. This resulted in half-life values greater than about 630 Ga, and the measurements reported in [32, 33, 35, 38−43] needed to be corrected therefore for the 15% abundance of the emitting isotope [61]. The major discrepancy (a factor ~2) is noted between the results quoted in [35] and [39], both obtained in 1934.

Significant developments in the methodologies for detection of the alpha-particles emitted from nuclei and in the related energy measurements have been achieved in the last decades. The new technologies, combined with the ability to produce very thin films of Sm and Sm-oxide, constrain the measured half-life values of ^{147}Sm around 110 Ga, with associated uncertainties varying from ~ 0.8% [57] to 4.0% [34]. It had to be noted that the measurements yielding values of $T_{1/2}$ < 130 Ga have been performed mainly after 1950 (twenty-four data), only three measurements of $T_{1/2}$ < 130 Ga have been obtained before 1950 [35, 38, 43].

Disregarding older measurements (those obtained before 1950), the data of Table 1 have been arranged into five groups of half-life-values according to

the different experimental techniques with which they were obtained (ionization chamber-IC, proportional counter-PC, liquid scintillation counter-SC, silicon surface-barrier detector-SB, and visual track detectors-VD (nuclear emulsion and dielectric plastic CR-39 plates).

An analysis of these data shows that all five groups of measurements exhibit two modes of half-life-values (single or weighted average), *viz.*, a lower one [IC: (107.0 ± 0.8) Ga; PC: (105 ± 4) Ga; SC: (106.7 ± 0.7) Ga; SB: (106.5 ± 0.7) Ga; VD: (106 ± 4) Ga], and a higher mode [IC: (114 ± 2) Ga; PC: (125 ± 6) Ga; SC: (115 ± 2) Ga; SB: (115.8 ± 1.7) Ga; VD: (115 ± 3) Ga]. Such data show that the weighted average of the lower mode of all five techniques gives (106.7 ± 0.4) Ga ($\boldsymbol{\chi_\nu^2}$ = 0.11), whereas the higher mode of half-life varies between 114 and 125 Ga.

Following Begemann *et al.* [61], who affirmed that the half-life of ^{147}Sm determined by a totally independent geochronological inter-comparison method is consistent with a value of ~106 Ga [5, 55], it is the lower mode of half-life that can lead to the most probable half-life-value of ^{147}Sm. Thus, by combining the five lower mode results listed above with two half-life determinations by geochronological inter-comparisons [5, 55] (see Table 1) one has, finally, $T_{1/2}$ = (106.3 ± 0.5) Ga, with ~ 0.47% uncertainty (2σ) and $\boldsymbol{\chi_\nu^2}$ = 0.07.

3. Semi-empirical evaluation of half-life of ^{147}Sm isotope

The calculation model described in the Appendix has been used to estimate the half-life of ^{147}Sm isotope provided that an accurate and precise value for the model parameter *g* becomes available. This can be achieved from an isotope that exhibits alpha transitions with characteristics very similar to those of ^{147}Sm isotope. Moreover, such an alpha-radioactive isotope must be characterized by very small uncertainties on both the measured Q_α-value and alpha-decay half-life, $T_{1/2}$. Fortunately, we have found in the literature the case for ^{215}Po isotope, which fulfills such requirements. As a matter of fact, the precision of Q_α-value for ^{215}Po is 0.04 %. The recommended half-life-value, with a branching ratio of 0.99934 for the ground-state transition into the ground-state of the daughter nucleus ^{211}Pb, $T_{1/2}$ = (1.781 ± 0.004) ms, is also known with high precision [66].

In addition, ^{215}Po and ^{147}Sm isotopes show a number of similar nuclear characteristics such as; *i*) naturally occurring isotopes; *ii*) even-odd type nuclei; *iii*) small, or very small, degree of nuclear deformation; *iv*) practically 100% of branching ratio to α-transition into ground-state of their respective daughter nuclei; *v*) same high-spin and parity for both parent and daughter nuclei ($9/2^+$ for ^{215}Po and ^{211}Pb, and $7/2^-$ for ^{147}Sm and ^{143}Nd) leading to α-transitions of null angular momentum ($\ell = 0$). In this sense, ^{215}Po isotope may be considered as a suitable (indeed unique) partner of ^{147}Sm, and the *g*-value that can be extracted from the alpha-decay data of ^{215}Po is the most appropriate and precise *g*-value to estimate the half-life of ^{147}Sm.

Going on following the lines of the present calculation method (see Appendix), the semi-empirical *g*-value and its uncertainty, δg, are thus obtained as (equation (A15))

$$g = \frac{\tau_e - \tau_0 - \tau_2}{\tau_1}, \delta g = \frac{\sqrt{(\delta\tau_e)^2 + (\delta\tau_0)^2 + (g\delta\tau_1)^2 + (\delta\tau_2)^2}}{\tau_1}. \quad (1)$$

Here, $\tau_e = \log T_{1/2}$ denotes the decimal logarithm of the experimental half-life, and $\delta\tau_e$ is its associated uncertainty (other quantities in equation (1) have been defined in the Appendix [see equations (A17)−(A22)]).

The nuclear quantities for ^{215}Po to be used in the present calculation are

Q_α = (7.561955 ± 0.003100) MeV, c = 8.798 fm, a = 5.602 fm,

μ_0 = 3.92701 u, z = 0.281723, $T_{1/2}$ = (1.782 ± 0.004) ms (ground-state into ground-state α-transitions), from which one obtains

$$g = 0.09326 \pm 0.00129. \quad (2)$$

In order to evaluate the half-life for ^{147}Sm isotope and the associated uncertainty, the nuclear data are: Q_α = (2.333269 ± 0.001937) MeV, c = 7.995 fm, a = 4.809 fm, μ_0 = 3.892491 u, and z = 0.107957.

Finally, by using the *g*-value given in (9), the half-life for ^{147}Sm isotope results to be

$$T_{1/2} = (108.2 \pm 3.0)\ \text{Ga}. \quad (3)$$

An insight into the present model reveals interesting aspects of the alpha-decay process. By evaluating the different contributions (λ_0, S, and P) to the

decay constant λ (equation (A3)), it is found that for nuclei with very similar nuclear characteristics, such as ^{215}Po and ^{147}Sm, the λ_0- and S-values appear to be very much the same. Thus, the decay constant (or half-life) is, in this case, dictated essentially by the penetrability factor P through the external Coulomb potential barrier in the separation region (see figure in Appendix). This behavior is shown in Table 2, which lists the λ_0-, S-, and P-values for both the ^{215}Po and ^{147}Sm isotopes. It is seen that both the "knocking frequency" λ_0 and the alpha-particle preformation probability S, are practically the same. Conversely, the "tunneling" through the external barrier, P, differs from each other isotope by many orders of magnitude, in such a way that P and $T_{1/2}$ result to be quantities inversely proportional ($P{\cdot}T_{1/2} \approx$ constant).

Table 2. Values of the different quantities that compose the alpha-decay half-life

α – emitter nuclide	Knocking frequency[a] $\lambda_0[10^{21}\mathrm{s}^{-1}]$	Preformation probability[b] S	Penetrability through the external barrier[c] P	Half-life[d] $T_{1/2}$
^{215}Po	1.7205	0.3215	0.703 x 10^{-18}	1.782 ms
^{147}Sm	1.1182	0.3243	5.600 x 10^{-40}	108.2 Ga

[a] $\lambda_0[10^{21}\mathrm{s}^{-1}] = 6.945694\frac{1}{a}\sqrt{\frac{Q_\alpha}{\mu_0}}$; [b] $S = 10^{-g\tau_1}$; [c] $P = 10^{-\tau_2}$; [d] $T_{1/2} = \frac{\ln 2}{\lambda_0 SP}$

As concerns alpha-transitions from the ground-state of ^{147}Sm into the first excited state of ^{143}Nd at 0.74204 MeV, with spin and parity $3/2^-$, such transitions would be very unlikely to occur due to both *i*) a significant reduction in the full Q_α-value and *ii*) the mutual angular momentum $\ell = 2$, which comes from the spin and parity $7/2^-$ of ^{147}Sm parent nucleus. This latter creates an additional centrifugal potential barrier in the separation region of fragments, while the former, coupled with a higher barrier, leads to an extremely low penetrability factor, therefore making such transitions not accessible to experimental observation.

4. Discussion and conclusions

The search for an accurate determination of ^{147}Sm half-life was prompted by the increased interest in exploiting the radioactivity of long-term decaying nuclides for geochronological applications. In this context we

were encouraged to re-analyze in a critical way the whole set of available experimental values of ^{147}Sm half-life.

The compilation of the half-life data reported along with the indication of the used technique allowed us to draw some interesting considerations. Half-life values obtained after 1950, when experimentalists did take into consideration the isotopic percentage of ^{147}Sm in ^{nat}Sm, are found to range between (104 ± 3) Ga [50] and (125 ± 6) Ga [36]. Among such data, the highest value was found by using a proportional counter, whereas the lower one by using a liquid scintillation counter. The uncertainties associated with the experimental determinations are in the range 1−6 Ga.

Several experimental factors can affect the measurements. As noted by Wilsenach *et al.* [34], who used techniques typical of materials science, the nature of the sample holder can influence the results. Their final half-life-value, (107.9 ± 2.6) Ga, was derived by weighting half-life determinations ranging between (106.9 ± 1) Ga and (115.4 ± 3.4) Ga, and by combining the results of different runs performed with the use of the same holder.

Other researchers were not so detailed in investigating the possible sources of random and/or systematic errors. So, it is not possible, for example, to find out if the somewhat high values of (117 ± 2) Ga and (115 ± 2) Ga measured in the last decade by Kinoshita *et al.* [56], or (125 ± 6) Ga reported in [36], could be ascribed to peculiar features of the experiments, such as the design and/or thickness of the Sm targets . The statistical analysis must, therefore, be undertaken without any possibility to eliminate, from the beginning, data that could be affected by systematic errors.

In this context, we have treated the twenty-four data of the last seven decades by classifying them according to the different techniques of measurements, at the same time taking advantage of results that had been obtained by a completely independent method, the geochronological inter-comparison. As summarized at the end of section 2, we have reached in this way the value (106.3 ± 0.5) Ga for the half-life of ^{147}Sm.

To confirm such a result, we felt it worthwhile to undertake an evaluation of the ^{147}Sm half-life using a close formula based on a previously proposed one-parameter, semi-empirical model for alpha emission from nuclei. We remark that, for the present application, the routine calculation of the model has been up-dated by inserting the most recent values of nuclear data

[67,68]. From the calculation model described in the Appendix and used in the precedent section a value of (108.2 ± 3.0) Ga has been obtained for half-life of ^{147}Sm.

The remarkable result of the present investigation is the quite good agreement found between the half-life evaluated by using the present one-parameter model and the one evaluated from a detailed analysis of the twenty-four significant results obtained after 1950 (listed in Table 1) . This allows us to safely rule out the weighted average (114 ± 2) Ga (2σ) of the nine higher half-life determinations of ^{147}Sm, therefore the result (106.3 ± 0.5) Ga (2σ) can now be regarded as the recommended half-life value of ^{147}Sm for geo- and cosmo-chronological determinations.

To conclude, the evaluation of alpha-decay half-life by applying our already successfully tested semi-empirical model based on a tunneling mechanism seems a reliable way to assess the validity of experimental half-life values of other alpha-active isotopes of interest to a number of useful applications in science and technology.

Acknowledgments

The authors wish to express their gratitude to Dr. Igor M. Villa for his utmost important and valuable comments, criticism, and the deep discussion on the treatment of the data as well. The kind cooperation by J. G. T. Monteiro in preparing the figure and tables is also gratefully acknowledged.

APPENDIX

A semi-empirical, calculation model to evaluate alpha-decay half-life

A semi-empirical, one-parameter model to estimate the half-lives of bismuth isotopes was developed by us in 2005 [62]. Subsequently, the model was also successfully applied not only to a large number of alpha radioactive decays [69−71] , but also to proton radioactivity [72−73] and to the spontaneous emission of heavy clusters from nuclei [74−75].

The proposed calculation method is based on the current quantum mechanical tunneling mechanism through a potential barrier, introduced in

late 1920's by Gamow, Gurney and Condon [76−78]. Here, a Coulomb-plus-centrifugal-plus-overlapping potential barrier has been considered within the spherical nuclear shape approximation. A schematic model of the alpha-particle tunneling through a potential barrier in the radioactive decay of ^{147}Sm is illustrated in Fig. A1.

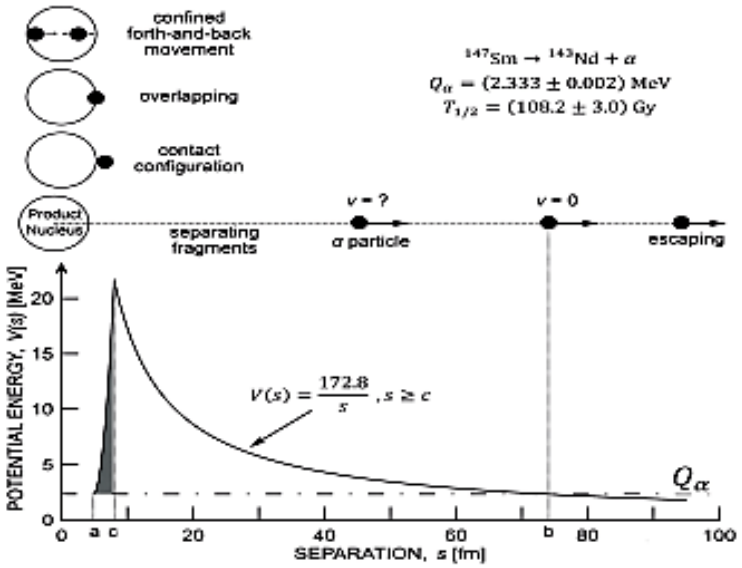

Fig. A1. Alpha-particle tunneling through a potential barrier in the radioactive decay of ^{147}Sm isotope. The shaded area emphasizes the overlapping region $a-c$. In the external separation region $c-b$ the full line represents the Coulomb potential barrier, and the Q_α-value (evaluated from nuclear masses) is indicated by the dash-dotted line. In the upper part the steps of the alpha-particle emission mechanism are schematically shown around the common center-of-mass; at $s = b$ the alpha-particle begins to escape from the atom at rest.

The case investigated in the present study, *i.e.* the alpha-decay of ^{147}Sm parent (P) isotope, does not exhibit centrifugal effects associated with the rotation around their common center-of-mass of the nuclei produced by disintegration: the alpha particle (α) and the ^{143}Nd daughter (D) isotope. This effect comes from the conservation laws

$$\boldsymbol{J}_\mathrm{P} = \boldsymbol{J}_\mathrm{D} + \boldsymbol{J}_\alpha + \boldsymbol{\ell}, \quad \boldsymbol{\pi}_\mathrm{P} = \boldsymbol{\pi}_\mathrm{D}\cdot\boldsymbol{\pi}_\alpha(-1)^{\ell} \tag{A1}$$

of spin ($\boldsymbol{J}$) and parity ($\boldsymbol{\pi}$) applied to the transition

$$^{147}\mathrm{Sm}\ (\boldsymbol{J}^{\pi} = 7/2^{-}) \rightarrow {}^{143}\mathrm{Nd}\ (\boldsymbol{J}^{\pi} = 7/2^{-}) + {}^{4}\mathrm{He}\ (\boldsymbol{J}^{\pi} = 0^{+}) \tag{A2}$$

which give $\ell = 0$ for the mutual angular momentum**.** In addition, the alpha decays are ground-state into ground-state transitions, so that

the total disintegration energy of the decay process, the Q_α-value, is entirely converted into kinetic energy of the product nuclei. The main ideas and assumptions of the model are here described briefly.

The decay constant, λ, is given by the product of three quantities, namely,

$$\lambda = \lambda_0 SP, \quad S = \exp(-G_{\rm ov}), \quad P = \exp(-G_{\rm se}), \tag{A3}$$

in which λ_0 represents the number of assaults on the potential barrier per unit time, S is the alpha-particle preformation probability, *i.e.*, the chance to find the alpha particle at the nuclear surface of the daughter nucleus, and P is the penetrability factor through the external Coulomb barrier created by the alpha particle and the daughter nucleus. The frequency factor λ_0 is commonly evaluated as

$$\lambda_0 = \frac{v}{2a} = \frac{\sqrt{2}}{2a}\sqrt{\frac{Q_\alpha}{\mu_0}}, \tag{A4}$$

where v is the relative velocity of the fragments in their forth and back movement, μ_0 is the reduced final mass of the separating fragments and $a = R_{\rm P} - R_\alpha$ is the extension of the overlapping region. $R_{\rm P}$ and R_α represent the radius of the parent nucleus and of the alpha particle, respectively (see figure). In equation (A3), the G's are the semi-classical WKB-integral approximation, known as Gamow's factor for decay, given by

$$G = \left(\frac{2}{\hbar}\right)\int_{s_1}^{s_2}\sqrt{2\mu(s)[V(s) - Q_\alpha]}\,{\rm d}s. \tag{A5}$$

Here, s represents the separation between the centers of the fragments, $V(s)$ is the potential barrier, and $\mu(s)$ is the reduced mass of the disintegrating system. $G_{\rm ov}$ is obtained in the overlapping barrier region, where the alpha particle to be emitted drives away from the position at $s_1 = a$ to the contact configuration at $s_2 = c = R_{\rm D} + R_\alpha$ (see figure). $R_{\rm D}$ denotes the radius of the daughter nucleus. The quantity $S = \exp(-G_{\rm ov})$ represents, therefore, the probability of the alpha particle to be found at the nuclear surface of the daughter nucleus. The result for $G_{\rm ov}$ reads

$$G_{\rm ov} = \frac{2}{\hbar}\,(c-a)g\,\sqrt{2\mu_0 Q_\alpha}\,\sqrt{\frac{1}{z} - 1}, \quad z = \frac{cQ_\alpha}{2e^2 Z_{\rm D}}, \tag{A6}$$

in which e^2 is the square of the electronic elementary charge, $\hbar$ is Planck's constant, and g is the model parameter to be found semi-empirically (see below).

G_{se} is calculated through the external, separation barrier region (only Coulomb potential barrier when $\ell = 0$) which extends from $s_1 = c$ up to the position $s_2 = b$, where the potential energy equals the Q_α-value, *i.e.*, $V(b) = Q_\alpha$ (see figure). In this barrier region, the effective reduced mass of the separating fragments, μ_0, is constant and given by $\mu_0^{-1} = m_D^{-1} + m_\alpha^{-1}$, where the m's denote the nuclear (rather than atomic) masses of the daughter nucleus and of alpha particle. Starting from equation (A5), the G-factor in the separation region results

$$G_{se} = 4\sqrt{2}\,\frac{e^2}{\hbar} Z_D \sqrt{\frac{\mu_0}{Q_\alpha}} \cdot F(z), F(z) = \arccos\sqrt{z} - \sqrt{z(1-z)}. \qquad \text{(A7)}$$

By combining equations (A3), (A4), (A6) and (A7), the half-life, $T_{1/2} = \ln(2)/\lambda$, is obtained as

$$T_{1/2} = \frac{\ln 4}{\sqrt{2}}\, a \sqrt{\frac{\mu_0}{Q_\alpha}} \cdot \exp(G_{ov} + G_{se}). \qquad \text{(A8)}$$

The semi-empirical character of the present calculation method is due to the presence of a unique adjustable parameter, g, related to the strength of the probability for alpha particle preformation through the quantity $\exp(-G_{ov})$ (see equation (A6).

The g parameter is given by a combination of the exponents p and q in the power functions that describe the reduced mass, $\mu(s)$, and the potential barrier, $V(s)$, respectively, in the overlapping region ($a \leq s \leq c$) [62] ,

$$g = \left(1 + \frac{p+q}{2}\right)^{-1}, \; 0 < g \leq 2/3. \qquad \text{(A9)}$$

The semi-empirical g-value depends on the source of input data for both nuclear mass and radius, on the adopted values for the different physical constants, and, of course, on the measured half-life for a given alpha-emitter nuclide or a set of alpha decay cases. Accordingly, the sources of the basic data for the alpha-decaying nuclides must be specified. Once a mass table and/or a nuclear radius parametrization were chosen, subsequent half-life evaluations should be done using these sources for mass- and radius-values, as well as the physical constants from which the g-value was obtained.

In the present work option was for the use of the AME2016 mass tables by Wang *et al.* [67] in order to evaluate the Q_α-values and the effective reduced mass, μ_0. These quantities are given by

$$Q = m_{\mathrm{P}} - (m_{\mathrm{D}} + m_\alpha), \qquad \mu_0^{-1} = m_{\mathrm{D}}^{-1} + m_\alpha^{-1}, \qquad \text{(A10)}$$

where the m's represent the nuclear (rather than the atomic) mass, which are calculated by the usual way, namely,

$$m_i = A_i - Z_i \cdot m_e + \left(\Delta M_i + kZ_i^\beta\right)/F, \quad i = \mathrm{P,D}. \quad \text{(A11)}$$

Here, m_e = 0.54857990907×10^{-3} u is the electron rest mass, m_α = 4.001506179127 u is the alpha particle mass, ΔM_i's are the atomic mass-excess values (expressed in MeV) as tabulated in [67], $k{\cdot}Z_i^\beta$ represents the total binding energy of the Z electrons in the atom, and F = 931.4940038 MeV/u is the mass-energy conversion factor. The k- and β-values come from an analysis of calculated data for electron binding energies of neutral atoms by Huang *et al*. [79]. From the analysis one obtains

$$k_1 = 8.7{\times}10^{-6} \text{ MeV and } \beta_1 = 2.517 \text{ for } Z \geq 60 \text{ nuclei,} \qquad \text{(A12)}$$

$$k_2 = 13.6 \times 10^{-6} \text{ MeV and } \beta_2 = 2.408 \text{ for } Z < 60 \text{ nuclei.} \qquad \text{(A13)}$$

The Q_α-value (expressed in MeV) is therefore given by

$$Q_\alpha = \Delta M_{\mathrm{P}} - (\Delta M_{\mathrm{D}} + \Delta M_\alpha) + \left[k_1\left(Z_{\mathrm{P}}^{\beta_1} - Z_{\mathrm{D}}^{\beta_1}\right) - 72.18 \cdot 10^{-6}\right], \quad \text{(A14)}$$

where the term in brackets represents the effect of the screening of the nucleus due to the surrounding electrons. The use of k_1 and β_1 in (A14) is because we are dealing with nuclei of $Z \geq 60$.

The nuclear radius values for the parent and daughter nuclei were evaluated following the finite range droplet model of atomic nuclei as is described by Möller *et al.* [80], and adopting the spherical approximation of the nuclear volume. The expressions that enable to calculate the average equivalent root-mean-square radius of the proton and neutron density distributions, $\overline{R}$, can be found in Refs. [62, 70, 75]. It is remarked that the reduced equivalent liquid drop nuclear radius ($r_0 = \bar{R}/A^{1/3}$) reveals a small, but important, decrease when one passes from intermediate-mass nuclei ($r_0 \approx$ 1.22 fm) to heavy ones ($r_0 \approx$ 1.20 fm). This indicates a clear degree of nuclear compressibility and makes, therefore, the simple expression R =

$r_0A^{1/3}$ not valid in estimating the radius for nuclei in the whole range of mass number.

Concerning the alpha-particle radius, for its equivalent sharp radius the value R_α = (1.62 ± 0.01) fm has been adopted. This radius value has been derived from the charge density distribution measured by Sick *et al*. [81] by performing electron scattering experiments on ^{4}He. Excellent reproducibility of alpha-decay data was attained using the above mentioned R_α-value coupled with a simple Gamow's-like model applied to a large number (more than three hundred cases) of measured alpha-decay half-lives covering the mass-number interval $106 \leq A \leq 264$ [70].

Finally, by expressing lengths in fm, masses in u (atomic mass unit), energies in MeV, half-life in Ga (1Ga = 10^9 a)**,** and, for convenience, taking decimal logarithm in equation (A8), we have

$$\tau = \log T_{1/2}\,[\mathrm{G}y] = \tau_0 + g\tau_1 + \tau_2, \tag{A15}$$

$$\tau_0 = -38.4999859 + \log\left(a\sqrt{\frac{\mu_0}{Q_\alpha}}\right), \tag{A16}$$

$$\tau_1 = 0.19\,(c-a)\sqrt{\mu_0 Q_\alpha}\sqrt{\frac{1}{z}-1}, \tag{A17}$$

$$\tau_2 = 0.5471604\,Z_\mathrm{D}\sqrt{\frac{\mu_0}{Q_\alpha}}\cdot F(z). \tag{A18}$$

The uncertainties associated with the quantities $\tau_0, \tau_1,$ and τ_2 come essentially from the uncertainty δQ_α associated with the Q_α-value, and are calculated as

$$\delta\tau_0 = 0.21714\,\delta Q_\alpha/Q_\alpha, \tag{A19}$$

$$\delta\tau_1 = 0.01805(c-a)^2\mu_0\,\delta Q_\alpha/\tau_1, \tag{A20}$$

$$\delta\tau_2 = K_1K_2^{3/2}\left[\frac{\arccos\sqrt{z}}{\sqrt{z}} + \frac{\sqrt{1-z}}{2z}\right]\cdot\delta Q_\alpha, \tag{A21}$$

in which

$$K_1 = 0.5471604\,Z_\mathrm{D}\sqrt{\mu_0} \text{ and } K_2 = z/Q_\alpha. \tag{A22}$$

References

[1] American Physical Society - A Report by the APS Panel on Public Affairs 2011 "Energy Critical Elements: Securing Materials for Emerging Technologies" (Washington, DC, USA)

[2] European Commission - Report of the *Ad-hoc* Working Group on Defining Critical Raw Materials 2011: Communication from the Commission to the European Parliament , the Council, the European Economic and Social Committee and the Committee of the Regions on the 2017 list of Critical Raw Materials for the EU (COM/2017/0490)

[3] Japan Oil, Gas and Metals National Corporation: "Rare Metals Stockpiling": http://www.jogmec.go.jp/english/stockpiling/stockpiling_10_000001.html

[4] Lugmair G W 1974 Sm-Nd ages: a new dating method *Meteoritics* **9** 369

[5] Lugmair G W and Marti K 1978 Lunar initial $^{143}Nd/^{144}Nd$: differential evolution of the lunar crust and mantle *Earth Planet. Sci. Lett.* **39** 349

[6] Hamilton P J, Evensen N M and O'Nions R K, Smith H S and Erlank A J 1979 Sm-Nd dating of Onverwacht Group Volcanics, Southern Africa *Nature* **279** 298

[7] Humphries F J and Cliff R A 1982 Sm-Nd dating and cooling history of Scourian granulites, Sutherland *Nature* **295** 515

[8] Chesley J T, Halliday A N and Scrivener R C 1991 Samarium-Neodymium direct dating of fluorite mineralization *Science* **252** 949

[9] Bros R, Stille P, Gauthier-Lafaye F, Weber F and Clauer N 1992 SmNd isotopic dating of Proterozoic clay material: An example from the Francevillian sedimentary series, Gabon *Earth Planet. Sci. Lett.* **113** 207

[10] Boyet M, Carlson R W and Horan M 2010 Old Sm-Nd ages for cumulate eucrites and redetermination of the solar system initial $^{146}Sm/^{144}Sm$ ratio *Earth Planet. Sci. Lett.* **291** 172

[11] Clayton R N 2007 Isotopes: From Earth to the Solar System. *Ann. Rev. Earth Planet. Sci.* **35** 1

[12] Clayton R N 2015 in *Encyclopedia of Scientific Dating Methods* Rink W J and Thompson J W (Eds.) Springer Science-Business (Dordrecht)

[13] Fowler W A and Hoyle F 1960 Nuclear Cosmochronology *Ann. Phys.* **10** 280

[14] Symbalisty E M D and Schramm D N 1981 Nucleocosmochronology *Rep. Prog. Phys.* **44** 293

[15] Takahashi K 1998 The ^{187}Re-^{187}Os cosmochronometry – the latest developments *AIP Conf. Proc*. **425** 616

[16] Hiess J, Condon D J, McLean N and Noble S R 2012 ^{238}U/^{235}U Systematics in Terrestrial Uranium-Bearing Minerals *Sci*. **335** 1610

[17] Wagner J K 1982 An overview of meteorite history as revealed by isotopic dating *Astron. Quart*. **4** 179

[18] Wilde S A, Valley J W, Peck W H and Graham C M 2001 Evidence from detrital zircons for the existence of continental crust and oceans on the Earth 4.4 Gyr *Nature* **409** 175

[19] A.N. Krot and M. Bizzarro 2009 Chronology of meteorites and the early solar system *Geochim. Cosmochim. Acta* **73** 4919

[20] Amelin Y, Kaltenbach A, Iizuka T, Stirling C H, Ireland T R, Petaev M and Jakobsen S B 2010 U–Pb chronology of the Solar System's oldest solids with variable ^{238}U/^{235}U *Earth Planet. Sci. Lett.* **300** 343

[21] Dauphas N and Chaussidon M 2011 A perspective from extinct radionuclides on a young stellar object: the Sun and its accretion disk *Ann. Rev. Earth Planet. Sci*. **39** 351

[22] Connelly J N, Bizzarro M, Krot A N, Nordlund A, Wielandt D and Ivanova M A 2012 The Absolute Chronology and Thermal Processing of Solids in the Solar Protoplanetary Disk *Science* **338** 651

[23] Amelin Y and Ireland T R 2013 Dating the oldest rocks and mineral in the solar system *Elements* **9** 39

[24] Frebel A, Christlieb N, Norris J E, Thom C, Beers T C and Rhee J 2007 Discovery of HE 1523-0901, a strongly r-process-enhanced metal-poor star with detected uranium *Astrophys. J.* **660** L117

[25] Brennecka G A, Borg L E and Wadhwa M 2013 Evidence for supernova injection into the solar nebula and the decoupling of r-process nucleosynthesis *Proc. Nat. Acad .Sci.* (USA) **110** 17241

[26] Lawrence C R 2015, JPL (for the Planck Collaboration) Astrophysics Subcommittee, NASA HQ

[27] Hidaka H and Yoneda S 2007 Sm and Gd isotopic shift of Apollo 16 and 17 drill stem samples and their implications for regolith history *Geochem. Cosmochem. Acta* **71** 1074

[28] Wasson J T 1985 *Meteorites: their record of early solar-system history* (Freeman W H and Co Ed., New York)

[29] Davis A M 2005 *Meteorites, Comets and Planets* Treatise of Geochemistry vol 1 (Oxford, Elsevier-Pergamon)

[30] Krot A N and Bizzarro M 2009 Contributions to the Workshop on Chronology of Meteorites and the Early Solar System (Kauai, Nov 5-7, 2007) *Geochem. Cosmochim. Acta* **73** (Suppl.) A1−A5

[31] Hevesy G and Pahl M 1933 Range of radiation from Samarium *Nature* **131** 434

[32] Hevesy G, Pahl M and Hosemann R 1933 Die Radioaktivität des Samariums *Z. Phys.* **83** 43

[33] Curie M and Joliot F 1934 Sur la radioactivité du samarium *Compt. Rend. Acad. Sci. (Paris)* **198** 360

[34] Wilsenach H, Zuber K, Degering D, Heller R, and Neu V 2017 High precision half-life measurement of ^{147}Sm α decay from thin-film sources *Phys. Rev.* C **95** 034618

[35]Libby W F 1934 Radioactivity of Neodymium and Samarium *Phys. Rev*. **46** 196

[36] Beard G and Wiedenbeck M L 1954 Natural radioactivity of Sm^{147} *Phys. Rev.* **95** 1245

[37] Mäder M 1934 Die Eigenschaften der Samarium-Strahlung *Z. Physik* **58** 601

[38] Lyford D 1934 The Radioactivity of Samarium *Thesis* The Johns Hopkins University

[39] Herszfinkiel M and Wroncberg A 1934 Radioactivity of Samarium *Compt. Rend. Acad. Sci. (Paris)* **199** 133

[40] Hosemann R 1936 Die Radioaktivität des Samariums *Z. Physik* **99** 405

[41] Bethe H A 1937 Nuclear Physics B. Nuclear Dynamics, Theoretical *Rev. Mod. Phys.* **9** 69 page 166

[42] Lattes C M G, Samuel E G and Cuer P 1947 Radioactivity of Samarium: use of the photographic plate to determine low concentrations of radioactive materials *An. Acad. Brasil. Cienc.* **19** 1

[43] Picciotto E 1949 Étude de la radioactivité du Samarium par la méthode photographique *Comp. Rend. Acad. Sci. (Paris)* **229** 117

[44] Leslie G E 1954 Thesis, North Carolina State College AD-37749; 1956 *Nucl. Sci. Abst.* **10** 134

[45] Beard G B and Kelly W H 1958 The use of a samarium-loaded scintillator for the determination of the half-life of Sm^{147} *Nucl. Phys.* **8** 207

[46] Karras M and Nurmia M 1960 Natural radioactivity of Samarium and Neodymium *Nature* **185** 601

[47] Wright P M, Steinberg E P and Glendenin L E 1961 Half-life of Samarium-147 *Phys. Rev.* **123** 205

[48] MacFarlane R D and Kohman T P 1961 Natural alpha radioactivity in medium-heavy elements *Phys. Rev.* **121** 1758

[49] Graeffe G and Nurmia M 1961 The use of thick sources in alpha spectrometry *Ann. Acad. Sci. Fenn.* A **6** 1-14

[50] Donhoffer D 1964 Bestimmung der Halbwertszeiten der in der Natur Vorkommenden Radioaktiven Nuklide Sm^{147} und Lu^{176} Mittels Flüssiger szintillatoren *Nucl. Phys*. **50** 489

[51] Valli K, Aaltonen J, Graeffe G, Nurmia M and Pöyhönen R 1965 Half-life of Sm-147: comparison of ionization and liquid scintillation results *Ann. Acad. Sci. Fenn.* A 6 **177**

[52] Gupta M C and MacFarlane R D 1970 The natural alpha radioactivity of Samarium *J. inorg. nucl. Chem*. **32** 3425

[53] Al Batania B and Janecke J 1987 Half-lives of long-lived alpha emitters *Radiochim. Acta* **42** 159

[54] Martins J B, Terranova M L and Correa M M 1992 Half-life for alpha-decay of ^{147}Sm *Nuovo Cimento* **105A** 1621

[55] G W Lugmair and S J G Galer 1992 Age and isotopic relationships among the angrites Lewis Cliff 86010 and Angra dos Reis *Geochim. Cosmochim. Acta* **56** 1673

[56] Kinoshita N, Yokoyama A and Nakanishi T 2003 Half-life of Samarium-147 *J. Nucl. Radiochem. Sci.* **4** 5

[57] Kossert K, Jörg G, Nähle O and Gostomski C L 2009 High-precision measurement of the half-live of ^{147}Sm *Appl. Radiat. Isotopes* **67** 1702

[58] Su J, Li Z H, Zhu L C, Lian G, Bai X X, Wang Y B, Guo B, Wang B X, Yan S Q, Zeng S, Li Y J, Li E T, Jin S J, Liu X, Fan Q W, Zhang J L, Jiang X Y, Lu J X, Lan X F, Tang X Z and Liu W P 2010 Alpha decay half-life of ^{147}Sm in metal samarium and Sm_2O_3 *Eur. Phys. J.* A **46** 69

[59] Ruark A and Fussler K H 1935 On the half-lives of Potassium, Rubidium, Neodymium and Samarium *Phys. Rev.* **48** 151

[60] Holden N E 1990 Total half-lives for selected nuclides *Pure & Appl. Chem*. **62** 941

[61] Begemann F, Ludwig K R, Lugmair G W, Min K, Nyquist L E, Patchett P J, Renne P R, Shih C -Y, Villa I M and Walker R J 2001 Call for an improved set of decay constants for geochronological use *Geochim. Cosmochim. Acta* **65** 111

[62] Tavares O A P, Medeiros E L and Terranova M L 2005 Alpha decay half-life of bismuth isotopes *J. Phys. G: Nucl. Part. Phys*. **31** 129

[63] Chisté V and Bé M M 2011 ^{147}Pm. Comments on evaluation of decay data *LNE-CEA/LNHB/V* (Table 2: Experimental values of ^{147}Sm half-life)

[64] Snelling A 2015 Determination of the radioisotope decay constants and half-lives of Samarium-147 (^{147}Sm) *Answers Res. J.* **8** 305

[65] Weaver B 1950 Mass assignment of natural activity of Samarium *Phys. Rev.* **80** 301

[66] Singh B *et al* 2013 Nuclear Data Sheets for A = 211 *Nucl. Data Sheets* **114** 661

[67] Wang M, Audi G, Kondev F G, Huang W J, Naimi S and Xu X 2017 The AME2016 atomic mass evaluation (II) Tables, graphs and references *Chin. Phys.* C **41** 030003

[68] Audi G, Kondev F G, Wang M, Huang W J and Naimi S 2017 The NUBASE2016 evaluation of nuclear properties *Chin. Phys.* C **41** 030001

[69] Tavares O A P, Terranova M L and Medeiros E L 2006 New evaluation of alpha decay half-life of ^{190}Pt isotope for the Pt-Os dating system *Nucl. Instrum. Methods Phys. Res.* B **243** 256

[70] Medeiros E L, Rodrigues M M N, Duarte S B and Tavares O A P 2006 Systematics of alpha-decay half-life: new evaluations for alpha-emitter nuclides *J. Phys. G: Nucl. Part. Phys.* **32** B23

[71] Tavares O A P and Medeiros E L 2011 Natural and artificial alpha radioactivity of Platinum isotopes *Phys. Scr.* **84** 045202

[72] Medeiros E L, Rodrigues M M N, Duarte S B and Tavares O A P 2007 Systematics of half-lives for proton radioactivity *Eur. Phys. J.* A **34** 417

[73] Tavares O A P and Medeiros E L 2010 Proton radioactivity: the case for ^{53m}Co proton-emitter isomer *Eur. Phys. J.* A **45** 57

[74] Tavares O A P, Roberto L A M and Medeiros E L 2007 Radioactive decay by the emission of heavy nuclear fragments *Phys. Scr.* **76** 375

[75] Tavares O A P and Medeiros E L 2012 A simple description of cluster radioactivity *Phys. Scr.* **86** 015201

[76] Gamow G 1928 Zur Quantentheorie des Atomkernes *Z. Phys.* **51** 204

[77] Gurney R W and Condon E U 1928 Wave mechanics and radioactive disintegration *Nature* **122** 439

[78] Gurney R W and Condon E U 1929 Quantum mechanics of radioactive disintegration *Phys. Rev*. **33** 127

[79] Huang K-N, Aoyagi M, Chen M H, Crasemann B and Mark H 1976 Neutral-atom electron binding energies from relaxed-orbital relativistic Hartree-Fock-Slater calculations $2 \leq Z$ 106 *At. Data Nucl. Data Tables* **18** 243

[80] Möller P, Nix J R, Myers W D and Swiatecki W J 1995 Nuclear ground-state masses and deformations *At. Data Nucl. Data Tables* **59** 185

[81] Sick I, McCarthy J S and Whitney R R 1976 Charge density of ^{4}He *Phys. Lett*. B **64** 33